Mamm Genome (2015) 26:248–256
DOI 10.1007/s00335-015-9566-y

A Cascade of epistatic interactions regulating teratozoospermia in mice

Keitaro Hirawatari[1,2] · Naoto Hanzawa[2] · Ikuo Miura[3] · Shigeharu Wakana[3] · Hideo Gotoh[1]

Received: 20 January 2015 / Accepted: 29 April 2015 / Published online: 12 May 2015

Abstract Infertility in humans and subfertility in domestic animals are two major reproductive problems. Among human couples, ~15 % are diagnosed as infertile, and males are considered responsible in about 50 % of the cases. To examine male fertility, various sperm tests including analyses of sperm morphology, sperm count and sperm mobility are usually performed. Teratozoospermia, a condition characterized by the presence of morphologically abnormal sperm, is considered as a symptom of infertility. B10.MOL-TEN1 (TEN1) mice (*Mus musculus*) show inherited teratozoospermia at high frequencies (~50 %). In this study, the polygenic control of teratozoospermia in the TEN1 strain was analysed. A quantitative trait loci analysis indicated three statistically significant loci, *Sperm-head morphology* 3 (*Shm3*; logarithm of the odds (LOD) score, 29.25), *Shm4* (LOD score, 6.80), and *Shm5* (LOD score, 3.58). These three QTL peaks were mapped to 24.3 centimorgans (cM) on chromosome 1, 32.0 cM on chromosome X, and 63.8 cM on chromosome 6, respectively. Another locus that is yet to be determined was also predicted. *Shm3* was found to be the major locus responsible for teratozoospermia, and a sequential cascade of interactions of the other three loci was apparent. These results are expected to help understand the mechanisms underlying reproductive problems in humans or domestic animals.

Introduction

Reproduction is a highly regulated process that requires coordination of the functions of numerous genes. Infertility affects 10–15 % of human couples, and a male factor is estimated to be involved in nearly half of these cases (Visser and Repping 2010). Among domestic animals, reproductive performance has been declining for a long time in dairy cows (Lucy 2001; Royal et al. 2008; Maas et al. 2009).

Approximately, 600 testis-specific protein-coding genes have been identified. Null mutations have been introduced in nearly 400 genes associated with spermatogenesis using knockout mouse technology (Matzuk and Lamb 2008; Jamsai and O'Bryan 2011; Massart et al. 2012). Information regarding genetic abnormalities in spermatogenesis obtained using reverse genetics approaches is expected to further help understand male infertility. Recent advances in genetics have paved the way for the development of effective methods to study male infertility and subfertility. Accordingly, the number of "repro" mouse strains produced by the JAX Reproductive Mutagenesis Program (Handel et al. 2006) has reached more than a hundred, and a number of genes responsible for male infertility and subfertility have been identified (http://reprogenomics.jax.org). The bidirectional approaches described above are intended to study infertility caused by a single gene. However, reproduction is temporally regulated by the coordinated action of a number of genes.

Electronic supplementary material The online version of this article (doi:10.1007/s00335-015-9566-y) contains supplementary material, which is available to authorized users.

✉ Hideo Gotoh
gotoh@affrc.go.jp

[1] Animal Genome Research Unit, Agrogenomics Research Center, National Institute of Agrobiological Sciences, 1-2 Owashi, Tsukuba, Ibaraki 305-8634, Japan

[2] Graduate School of Science and Engineering, Yamagata University, 1-4-12 Kojirakawa, Yamagata 990-8560, Japan

[3] Technology and Development Team for Mouse Phenotype Analysis, RIKEN BioResource Center, 3-1-1 Koyadai, Tsukuba, Ibaraki 305-0074, Japan

Our approach was also genetic, and the phenotype was polygenic. Previously, 17 strains of mice were surveyed to determine the frequency of abnormal sperm-head morphology, and B10.M/Sgn (B10.M) and B10.MOL-TEN1 (TEN1) strains were ranked first and second, with respect to the frequency of sperm-head morphological abnormalities (Gotoh 2010). Both strains of mice showed teratozoospermia, producing sperm cells displaying a wide variety of morphological abnormalities. Segregation analysis revealed that the sperm phenotype was heritable in both strains. The frequency of occurrence of each type of morphological abnormality varied among individuals (Gotoh et al. 2012; Hirawatari et al. 2015). Further quantitative trait loci (QTL) analysis and fine mapping of B10.M strain identified two causative loci, *Sperm-head morphology 1* (*Shm1*) on chromosome (Chr) 1 and *Shm2* on Chr 4 (Gotoh et al. 2012). As to male fertility capacities of the two strains, the B10.M strain showed low fecundity while the TEN1 strain was fully fertile (Hirawatari et al. 2015). The relationship between sperm-head morphology and male subfertility is yet to be established.

Sperm phenotype of TEN1 strain has been reported to be controlled by at least three responsible loci (Hirawatari et al. 2015). In this study, we analysed the genetic control of sperm-head morphological abnormalities in the TEN1 strain by QTL analysis using backcross males between TEN1 and C3H/HeN strains, and gene mapping using F2 intercross males.

Materials and methods

Mice

All the experimental procedures were approved by the Institutional Animal Care and Use Committee of the National Institute of Agrobiological Sciences. The identification code for the animal experiments in this study at the institute is H20-009. Animals were housed and cared for according to the guidelines established by the Committee. B10.MOL-TEN1 (TEN1) mice were provided by the RIKEN BioResource Center (Tsukuba, Ibaraki, Japan). C3H/HeNCrlCrlj (C3H) mice were purchased from Charles River Japan (Yokohama, Japan). B10.M/Sgn (B10.M) mice are maintained at our facility. The animals were maintained on a cycle of 12 h of light and 12 h of darkness under specific pathogen-free conditions. A commercial mouse diet and water were provided to them.

TEN1 strain

This strain was one of the congenic lines established at the National Institute of Genetics, Japan (Mishima, Shizuoka, Japan) to define *H2* alleles on Chr 17 in the Japanese wild mouse population (Shiroishi et al. 1982). The original donor was a wild non-inbred animal (*Mus musculus molossinus)*. The wild-derived *H2* allele was transmitted to B10 over twelve generations. Subsequently, this strain has been maintained via sibling breeding.

Sperm morphology tests

Sperm collection from the cauda epididymis and sperm counts were performed according to methods in the report on the mouse sperm morphology test (Wyrobek et al. 1983). Sperm samples were collected from 3- to 5-month-old male mice. The animals were deeply anesthetised using 8.0 % isoflurane for inhalation until death, following which the epididymides were dissected. To obtain sperm for assessing its morphology, the epididymis from one side was removed and sperm were transferred into 1 mL of phosphate-buffered saline (pH 7.0) with 0.1 % glucose. The sperm-head morphology test was performed by the method described previously (Gotoh et al. 2012). Briefly, 1–5 μL of the sperm suspension was spread on a glass slide, air dried, fixed using ethanol, and sperm morphology was observed by differential interference contrast microscopy (DMRXA2; Leica Microsystems, Cambridge, UK) (×400 magnification). Two independent samples, each containing at least 200 sperm cells, were analysed. The classification of sperm-head morphological abnormalities is shown in Supplementary Fig. S1.

Preparation of genomic DNA

Mouse tails were resuspended in 300 μL Tris buffer (50 mM, pH 7.8) containing 100 mM ethylenediaminetetraacetic acid (EDTA), 100 mM NaCl, and 1 % sodium dodecyl sulphate (SDS) (w/v). Proteinase K (Wako, Osaka, Japan) was then added to a final concentration of 500 μg/mL. The samples were incubated on a shaker (Thermomixer comfort; Eppendorf, Hamburg, Germany), at 1000 rotation per minute, overnight, at 56 °C. RNase A (Wako, Osaka, Japan) was then added to a final concentration of 10 μg/mL, and the samples were incubated for 1 h at 37 °C. Following this, 300 μL DNA-binding reagent containing 4.5 M guanidine hydrochloride (Wako, Osaka, Japan), 0.5 M potassium acetate (pH 5.0), and 40 mg/mL silica gel (Sigma-Aldrich #288519, St. Louis, MO, USA) was added to the samples. The samples were then mixed by shaking for 1 min to allow the DNA to bind to the silica gel. Silica gel particles were retrieved and washed three times with a solution containing 80 % ethanol (v/v), 10 mM potassium acetate (pH 5.0), and 20 μM EDTA. After air drying, the bound DNA was eluted from the silica gel using TE buffer (pH 8.0). DNA concentration was calculated indirectly on the basis of the absorbance at

260 nm measured using a UV spectrophotometer (GeneQuant; Pharmacia Biotech, Cambridge, UK).

Genotyping

A genome-wide scan was conducted using single nucleotide polymorphism (SNP) markers spaced at 10 cM for backcross (BC) males ($n = 176$) produced from a genetic cross of ♀TEN1 × ♂(♀C3H × ♂TEN1)F1 mice. The 103 SNP markers used for the QTL analysis are listed in Supplementary Table S1. The markers were chosen from the Mouse SNA database (http://www.broad.mit.edu/snp/mouse/) as described previously (Furuse et al. 2012). We also used microsatellite markers (Supplementary Table S2) for a detailed mapping analysis for F2 males ($n = 592$) produced from intercross of (♀C3H × ♂TEN1)F1 mice. Procedures were same as described earlier (Gotoh et al. 2012).

QTL analysis

QTL analysis was performed to identify loci controlling frequencies of sperm-head abnormalities using R software (ver. 3.1.3 available at http://www.rqtl.org/) and qtl package (ver. 1.35-6) (Browman et al. 2003; Browman and Sen 2009). Genetic model was estimated using 176 BC males. We carried out single locus scans to identify independent effect QTLs. Because distribution of the phenotype was not normal, sperm abnormality data were transformed using Johnson SU function of the JMP statistical software (ver. 12.0.0, SAS Institute Inc., Cary, NC, USA). However, truly normalized distribution was not obtained (Supplementary Fig. S2). LOD scores were computed at 2-cM intervals across the genome using the "EM" method in R/qtl. Independent effect QTLs were considered significant (suggestive) if they exceeded the 95 % (63 %) genome-wide adjusted threshold based on 1000 permutations for autosomes and on 22,849 permutations for X chromosome. The significant (suggestive) thresholds were 2.71 (1.74) and 2.81 (1.86) for autosomes and X chromosome, respectively. For significant QTLs, a location of a 95 % confidence interval (CI) was estimated by a decline of 1.5 LOD. Epistatic effects were investigated using the genome-wide all-pairs scans. The significant thresholds for the pairwise scans were obtained from 1000 permutations. Two significant pairs of QTLs, 24.3 cM on chromosome 1 and 29.0 cM on X chromosome, and 61.8 cM on chromosome 6 and 29.0 cM on X chromosome, were suggested. Because one of QTLs in both pairs was positioned on X chromosome, multilocus scans were not applicable in R/qtl package. We then used 592 F2 males for further analysis. Microsatellite markers which cover the 95 % CI of the significant QTLs on chromosome 1, 6, and X were picked up, and then F2 samples were genotyped. Discrimination between epistatic effects and additive effects was judged by the results obtained from "effectplot" function of R/qtl.

Gene mapping

In attempt to narrow the region of QTL loci, we observed phenotype/genotype relationship using F2 males. One reason to perform this approach was that multiple QTL function of R/qtl package does not usable for a locus on Chr X. The other reason was that the sperm abnormality phenotype is clearly judged "high" or "low" with small ambiguity in this case.

Results

Sperm-head morphological abnormalities

The TEN1 strain displayed teratozoospermia. A wide variety of sperm-head morphologies, including a shortened apical hook, a bent hook, spermatozoa with ectopic attachment of the flagella, and several types of amorphous heads, were observed (Supplementary Fig. S1). The mean frequencies of abnormal sperm were 50.2 % for TEN1 and 2.4 % for C3H.

QTL analysis: main effects

Three statistically significant LOD score peaks appeared: Chr 1 at 24.3 cM with a LOD score of 29.25, Chr 6 at 63.8 cM with a LOD score of 3.58, and Chr X at 32.0 cM with a LOD score of 6.80 (Fig. 1; Table 1). The locus on Chr 1 was considered to be the major locus for the trait, while the other two loci on Chr X and Chr 6 were considered to be the minor loci. We named these loci on Chrs 1, X, and 6 as *Sperm-head morphology 3* (*Shm3*), *Shm4*, and *Shm5*, respectively.

QTL analysis: epistasis

Pairwise genome scans estimated two candidates for significant interactions: Chr1 at 24.1 cM with Chr X at 31.5 cM, and Chr 6 at 61.8 cM with Chr X at 31.5 cM. LOD scores by R/qtl package (LOD_f, LOD_{fv1}, LOD_{int}, LOD_a, LOD_{av1}) for these interactions were (35.7, 8.81, 0.0462, 35.6, 8.76) for Chr 1:Chr X interaction, and (12.2, 4.61, 0.0166, 12.2, 4.59) for Chr 6:Chr X interaction. Graphical draws representing LOD scores by two-dimensional, two-QTL genome scan were also shown in Supplementary Fig. S3. We then used frequencies of sperm-head abnormalities of F2 males, and analysed estimated average frequency of abnormal sperm as a function of

genotype of a marker at responsible QTLs (Fig. 2). Epistatic interaction between *Shm3* on Chr 1 (represented by 1@24.3) and *Shm4* on Chr X (represented by X@32.0) was evident because $Shm4^{C3H/-}$ suppressed sperm abnormality only when *Shm3* genotype was homozygous for *B10.M* allele (Fig. 2a). Effect of *Shm5* on Chr 6 (represented by 663.8) differed depending on the genotype of *Shm4* (Fig. 2b).

Genetic model of inheritance

The frequencies of sperm-head abnormalities of a total of 592 F2 animals were rearranged according to their *Shm3*, *Shm4*, and *Shm5* genotypes, and analysed to estimate the roles of the three loci in inheritance. The results depicted in Fig. 3 and Table 2 summarise our understanding of the results. The *TEN1* allele at the *Shm3* locus ($Shm3^{TEN1}$) was considered to be the major locus for the high frequency of sperm-head abnormalities. It acts recessively because 97 % of heterozygotes and *C3H* homozygotes showed low frequencies of abnormalities. $Shm3^{TEN1/TEN1}$ homozygotes showed high and low sperm-head abnormality phenotypes. Both *Shm4* and *Shm5* were considered conditional loci because both loci act in specific genotypes. The *C3H* allele

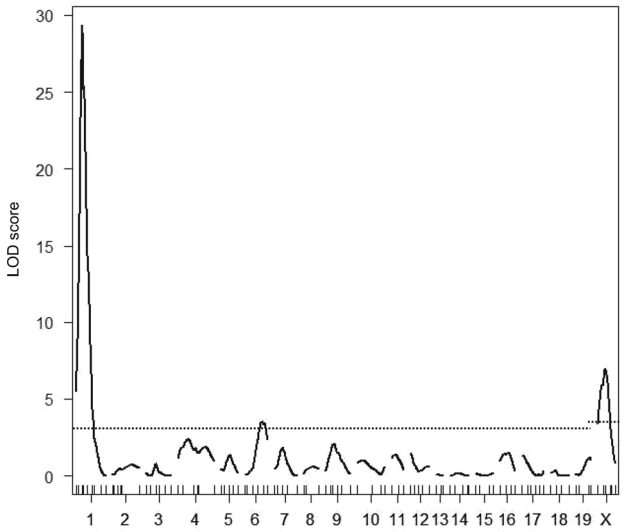

Fig. 1 Identification of the three loci responsible for the TEN1 sperm abnormalities phenotype by QTL analysis. Three statistically significant logarithms of the odds (LOD) score peaks appeared on Chrs 1, 6, and X. These peaks were found on Chr 1 at 24.6 cM with a LOD score of 29.25, on Chr 6 at 63.8 cM with a LOD score of 3.58, and on Chr X at 32.0 cM with a LOD score of 6.80. The statistically significant LOD threshold ($P = 0.05$) for the phenotype was 2.77 for autosomes and 2.81 for X chromosome (*a dotted horizontal line*), as determined by the permutation test ($n = 1000$) for autosomes and by the permutation test ($n = 22{,}849$) for X chromosome, respectively

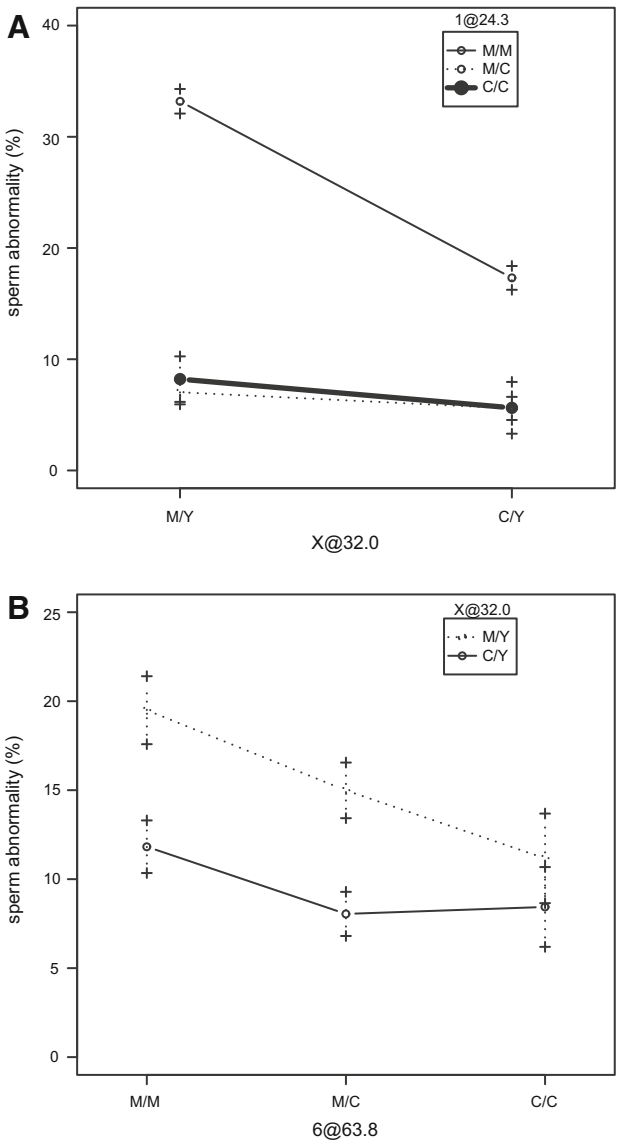

Fig. 2 Allele effects for frequency of abnormal sperm as a function of genotype at two putative QTL. **a** *Shm3* (1@24.3) and *Shm4* (X@32.0). **b** *Shm4* and *Shm5* (6@63.8). B10.M allele is represented by M, and C3H allele is represented by C. *y*-axes show mean values of sperm abnormality. *Error bars* represent SE

Table 1 QTLs identified for a single gene genome-wide scan

Chr	Locus name	LOD score	Peak (cM)	95 % CI (cM)	Nearest marker
1	*Shm3*	29.25	24.3	21.7–27.2	rs3022803
6	*Shm5*	3.58	63.8	45.8–84.9	rs3023094
X	*Shm4*	6.80	32.0	16.0–44.0	rs3695066

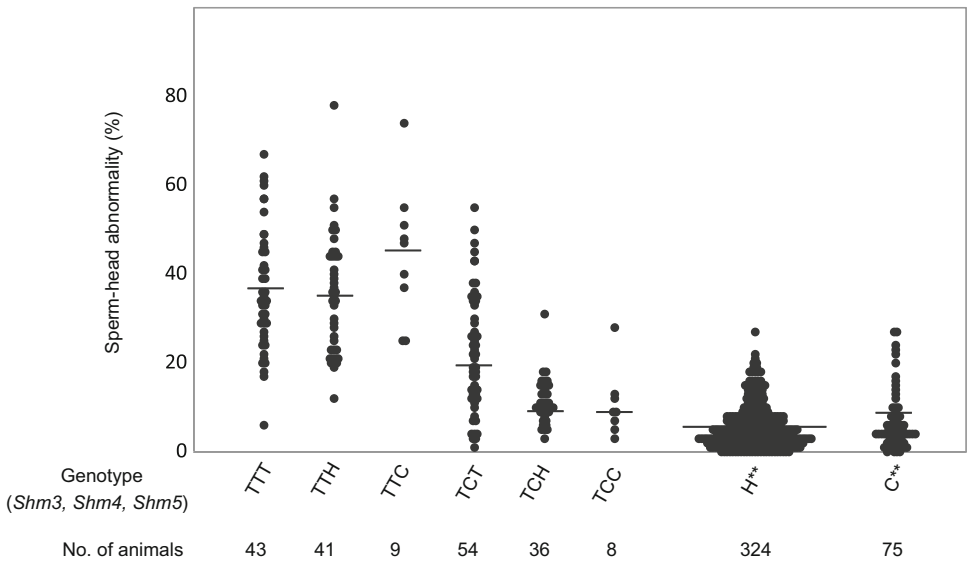

Fig. 3 Effects of *Shm3*, *Shm4*, and *Shm5* on sperm-head abnormalities. The frequency of sperm-head abnormalities of F2 animals ($n = 592$) was plotted for each genotype concerning the responsible loci *Shm3* on Chr 1, *Shm4* on Chr X, and *Shm5* on Chr 6. The genotypes of *D1Mit236*, *DXMit114*, and *D6Mit59* were used for the genotypes of the *Shm3*, *Shm4*, and *Shm5* loci, respectively. Each genotype is represented by three capital letters or stars. The first capital represents the genotype at the *Shm3* locus, the second represents the genotype at the *Shm4* locus, and the third represents the genotype at the *Shm5* locus. The homozygous state of autosomal *Shm3* and *Shm5* loci is shown as "T" from the TEN1 allele and as "C" from the C3H allele. The hemizygous state of the *Shm4* locus linked on Chr X is represented as "T" from the TEN1 allele and as "C" from the C3H allele. Heterozygotes are represented as "H". The star "*" represents "T" or "H" or "C". For example, the "TTT" represents an animal with the genotype $Shm3^{TEN1/TEN1}$, $Shm4^{TEN1/-}$, or $Shm5^{TEN1/TEN1}$. The genotype "TCT" was divided into two groups at 20 % of sperm-head abnormalities. The *horizontal bar* for each genotype represents the mean frequency of sperm-head abnormalities

Table 2 Expected function of QTL loci *Shm3*, *Shm4*, and *Shm5* in sperm-head morphological abnormalities

Shm3 genotype on Chr 1[a]	*Shm4* genotype on Chr X[a]	*Shm5* genotype on Chr 6[a]	Expected phenotype of sperm-head abnormality[b]	Observed phenotype[b]	Observed ratio (%)	No. of observed/total no.[c]
T	T	T or H or C	High	High	96	89/93
				Low	4	4/93
T	C	H or C	Low	High	4	2/46
				Low	96	44/46
T	C	T	High	High	52	28/54
				Low	48[d]	26/54
H or C	T or C	T or H or C	Low	High	3	11/399
				Low	97	388/399

[a] "T" denotes homozygous for the TEN1 allele for autosomes, and hemizygous for the TEN1 allele for Chr X. "C" denotes homozygous for the C3H allele for autosomes, and hemizygous for Chr X. "H" denotes heterozygous for the TEN1 and C3H alleles

[b] Quantitative threshold between "High" and "Low" was set at 20 %

[c] F2 hybrids ($n = 592$) were gathered for analysis

[d] Approximately, half of the animals did not show the expected phenotype. This may suggest involvement of another locus

of the *Shm4* locus on Chr X was considered to act in suppressing the action of $Shm3^{TEN1/TEN1}$ because 96 % of $Shm3^{TEN1/TEN1}$ and $Shm4^{TEN1/-}$ animals showed a high frequency of sperm-head abnormalities, and 96 % of $Shm3^{TEN1/TEN1}$, $Shm4^{C3H/-}$, $Shm5^{C3H/TEN1}$ and 96 % of $Shm3^{TEN1/TEN1}$, $Shm4^{C3H/-}$, $Shm5^{C3H/C3H}$ animals showed low frequency of sperm-head abnormalities (Fig. 3, Table 2). Animals with $Shm3^{TEN1/TEN1}$, $Shm4^{C3H/-}$, $Shm5^{TEN1/TEN1}$ showed high to low frequencies of abnormalities. Fifty-two percent of animals showed high frequency of abnormalities (≥20 %), and 48 % of animals showed low frequency of abnormalities (<20 %). We

considered that this genotype of animals could be divided into "High" and "Low" groups. Our understanding is that the $Shm5^{TEN1/TEN1}$ allele acts to suppress the action of $Shm4^{C3H/-}$ recessively, only when the genotype of *Shm3* is homozygous for the *TEN1* allele and the genotype of *Shm4* is *C3H*. From the information that 48 % of $Shm3^{TEN1/TEN1}$, $Shm4^{C3H}$, and $Shm5^{TEN1/TEN1}$ animals showed low frequency of abnormalities, another locus is expected to act in suppressing the action of $Shm5^{TEN1/TEN1}$.

Genetic mapping

Figure 4 shows the results of mapping the *Shm3*, *Shm4*, and *Shm5* loci. The *Shm3* locus was mapped between the *Ercc* marker (Chr 1: 23.55 cM) and the *D1Mit303* (Chr 1: 31.79 cM) marker. The *Shm4* locus was mapped between the *DXMit1* marker (Chr X: 37.29 cM) and the *DXMit170* marker (Chr X: 45.87 cM). The *Shm5* locus was mapped between the *D6Mit219* marker (Chr 6: 64.03 cM) and the *D6Mit14* marker (77.64 cM). Because the mapping results presented above were based on one recombinant in most cases, overinterpretation should be avoided.

Discussion

Several types of sperm tests, including sperm morphology, sperm count, sperm mobility, progressive motility, and others are used to assess male fertility (Aitken 2006; Lewis 2007; Oehninger et al. 2014). However, no reliable correlation between the results of sperm tests and observed fertility has so far been established (Guzick et al. 2001). Our study was intended to focus on genetic regulation of sperm morphology in mice as a model system to analyse the complicated reproductive regulation in mammals, including humans and domestic animals. In this study, we analysed the genetic regulation of the TEN1 strain for sperm-head morphological abnormalities.

In the previous study, the sperm phenotype of the TEN1 strain was found to be heritable, and was expected to be controlled by at least three loci (Hirawatari et al. 2015). Supporting the results of the segregation analysis, three statistically significant loci, *Shm3*, *Shm4*, and *Shm5*, were obtained from the QTL analysis. Locus mapping and further analysis determined the complicated genetic regulation by these three loci and another predicted locus on teratozoospermia. Together with our previous study on genetic teratozoospermia of B10.M strain (Gotoh et al. 2012), Fig. 5 shows our current understanding of the model representing the polygenic regulations of sperm-head abnormalities in TEN1 and B10.M. In both cases, complicated cascades of epistatic interactions were predicted. In the case of the TEN1 strain, the homozygosity of $Shm3^{TEN1}$ allele was confirmed to act as the major effect on teratozoospermia. It resembles the action of $Shm1^{B10.M}$ allele of B10.M. Sequential up- and down-regulations by *Shm4*, *Shm5*, and then by another predicted locus yet to be determined were estimated to constitute a cascade of interactions for teratozoospermia in TEN1 strain. Table 3 summarises the expected function of *Shm* loci obtained from both this study on TEN1 and our previous study on B10.M.

Coincidentally, the *Shm3* locus in TEN1 and the *Shm1* locus in B10.M were found to be located in the overlapping region on Chr 1. It may be that *Shm1* and *Shm3* encode the same gene. However, even if $Shm1^{B10.M}$ and $Shm3^{TEN1}$ are allelic, they certainly differ in their functional properties; $Shm4^{C3H}$ on Chr X interacts with $Shm3^{TEN1/TEN1}$ on Chr 1 suppressively, but it does not interact with $Shm1^{B10.M/B10.M}$ (Gotoh et al. 2012). Determination of genes encoded by both *Shm1* locus and *Shm3* locus would expected to clarify the issue.

$Shm4^{C3H}$ and $Shm4^{TEN1}$ were also found to differ in their functional properties (Table 3). $Shm4^{C3H/-}$ suppresses the action of $Shm3^{TEN1/TEN}$, while $Shm4^{TEN1/-}$ does not. Because TEN1 is an *H2* congenic strain on the background of B10 genome, sequence variation should be present between the genes encoded by $Shm4^{C3H}$ and $Shm4^{B10}$. Within the region between the *DXMit1* and *DXMit170* markers, polymorphic non-synonymous SNPs within the coding region between C3H/HeJ and C57BL/10J strains were searched for using the Mouse SNP query of the public database at the Jackson Laboratory (http://www.informatics.jax.org/javawi2/servlet/WIFetch?page=snpQF, Accessed Dec. 1, 2014). A total of 13 polymorphic genes and one synthetic QTL were found; *Tktl1*, *Llna*, *Gdi1*, *4930468A15Rik*, *4930595M18Rik*, *Heph*, *Stard8*, *Atrx*, *Atp7a*, *Hmgn5*, *Tex16*, *2010106E10Rik*, *Cpxcr1* genes, and *Hst3* QTL. These comprise the candidate genes encoded by *Shm4*. Interestingly, two male hybrid sterility QTL loci, *Hstx1* (Storchová et al. 2004) and *Mhysq2* (Vyskocilová et al. 2009), and one sperm-head anomaly locus, *Spha2* (Oka et al. 2004), have been mapped within the same region. The relationship between these loci and *Shm4* remains unknown.

No equivalent allele of $Shm2^{B10.M}$ on Chr 4, which enhance the action of $Shm1^{B10.M/B10.M}$, was found in the TEN1 genome. This may be because the $Shm2^{B10.M}$ locus contains a mutation that the TEN1 allele does not. Another possibility is that $Shm2^{B10.M}$ and $Shm2^{TEN1}$ are one and the same, and interact with $Shm1^{B10.M}$ but not with $Shm3^{TEN1}$.

Similarly, no equivalent allele of $Shm5^{TEN1}$ on Chr 6 was found in the B10.M genome. $Shm5^{TEN1}$ suppresses the action of $Shm4^{C3H/-}$ recessively, if the genotype is $Shm3^{TEN1/TEN1}$ and $Shm4^{C3H/-}$. From our research so far, it is not possible to predict the function of $Shm5^{B10.M}$.

At least one additional interacting locus involved in sperm-head abnormalities was predicted to exist in the genetic system analysed in this study. We expected the

A Shm3 locus mapping on chromosome 1

	Chr 1						Chr X			Chr 6					
DNA marker	Ercc5	D1Mit236	D1Mit235	D1Mit234	D1Mit528	D1Mit303	DXMit1	DXMit114	DXMit170	D6Mit219	D6Mit339	D6Mit59	D6Mit14	Abnormalities (%)	Animal No.
	T	T	T	T	T	T	T	T	T	T	T	T	T	57	244
	T	T	T	T	T	H	T	T	T	T	T	T	T	29	325
	H	H	H	H	H	T	T	T	T	T	T	T	T	5	412
	T	H	H	H	H	H	T	T	T	T	T	T	T	3	543
	H	H	H	H	H	H	T	T	T	T	T	T	T	1	337
	C	C	C	C	C	C	T	T	T	T	T	T	T	8	354

B Shm4 locus mapping on chromosome X

	Chr 1						Chr X			Chr 6					
DNA marker	Ercc5	D1Mit236	D1Mit235	D1Mit234	D1Mit528	D1Mit303	DXMit1	DXMit114	DXMit170	D6Mit219	D6Mit339	D6Mit59	D6Mit14	Abnormalities (%)	Animal No.
	T	T	T	T	T	T	T	T	T	H	H	H	H	48	246
	T	T	T	T	T	T	C	C	T	H	H	H	H	3	55
	T	T	T	T	T	T	T	T	C	H	H	H	H	34	350
	T	T	T	T	T	T	T	C	C	H	H	H	H	5	217
	T	T	T	T	T	T	T	C	C	H	H	H	H	16	389
	T	T	T	T	T	T	T	C	C	H	H	H	H	13	420
	T	T	T	T	T	T	T	C	C	H	H	H	H	11	429
	T	T	T	T	T	T	T	C	C	H	H	H	H	9	476
	T	T	T	T	T	T	C	T	T	H	H	H	H	45	231
	T	T	T	T	T	T	C	T	T	H	H	H	H	44	284
	T	T	T	T	T	T	C	T	T	H	H	H	H	36	367
	T	T	T	T	T	T	C	T	T	H	H	H	H	28	396
	T	T	T	T	T	T	C	T	T	H	H	H	H	44	419
	T	T	T	T	T	T	C	T	T	H	H	H	H	44	524
	T	T	T	T	T	T	C	C	C	H	H	H	H	5	41

C Shm5 locus mapping on chromosome 6

	Chr 1						Chr X			Chr 6					
DNA marker	Ercc5	D1Mit236	D1Mit235	D1Mit234	D1Mit528	D1Mit303	DXMit1	DXMit114	DXMit170	D6Mit219	D6Mit339	D6Mit59	D6Mit14	Abnormalities (%)	Animal No.
	T	T	T	T	T	T	C	C	C	T	T	T	T	45	60
	T	T	T	T	T	T	C	C	C	T	T	T	H	35	545
	T	T	T	T	T	T	C	C	C	T	T	T	H	22	615
	T	T	T	T	T	T	C	C	C	T	T	T	H	23	644
	T	T	T	T	T	T	C	C	C	T	H	H	H	9	115
	T	T	T	T	T	T	C	C	C	H	H	H	H	5	41
	T	T	T	T	T	T	C	C	C	C	C	C	C	9	240

Fig. 4 Fine mapping of *Shm3*, *Shm4*, and *Shm5* loci. The genotypes of the informative recombinants whose break points were mapped within the responsible genetic regions on Chr 1, X, and 6 are shown. **a** Fine mapping of the *Shm3* locus on Chr 1. **b** Fine mapping of the *Shm4* locus on Chr X. The genotype at the *Shm3* locus on Chr 1 had to be homozygous for the TEN1 allele. **c** Fine mapping of the *Shm5* locus on Chr 6. The genotype of the *Shm3* locus on Chr 1 had to be homozygous for the TEN1 allele, and the genotype of the *Shm4* locus on Chr X had to be hemizygous for the C3H allele. Homozygotes for the TEN1 allele, heterozygotes, and homozygotes for the C3H allele are represented as T, H, and C, respectively. The *dark shadowed regions* represent the presence of the responsible loci on the TEN1 chromosomes for the *Shm3* and *Shm5* loci, and represent the presence of the responsible locus on the C3H chromosome for the *Shm4* locus. The *light shadowed* chromosomal regions represent the absence of the responsible loci. The frequency of sperm-head abnormalities and the animal identification number are depicted to the right

Table 3 Estimated function of alleles at sperm-head morphology loci

Locus^{allele}	Chr	Location (cM)	Function in sperm-head abnormalities
[a]*Shm1*$^{B10.M}$	1	23.7	High frequency of sperm-head abnormalities. Recessive
[a]*Shm1*^{C3H}	1	23.7	No effect
[a]*Shm2*$^{B10.M}$	4	70.4	Enhance action of *Shm1*$^{B10.M/B10.M}$
[a]*Shm2*^{C3H}	4	70.4	No effect
Shm3^{TEN1}	1	24.3	High frequency of sperm-head abnormalities. Recessive
Shm3^{C3H}	1	24.3	No effect
Shm4^{TEN1}	X	32	No effect
Shm4^{C3H}	X	32	Suppress action of *Shm3*$^{TEN1/TEN1}$ hemizygously
Shm5^{TEN1}	6	63.8	Suppress action of *Shm4*$^{C3H/-}$ when the genotype is *Shm3*$^{TEN1/TEN1}$ and also *Shm4*$^{C3H/-}$. Recessive
Shm5^{C3H}	6	63.8	No effect
Unknown	ND	ND	Suppress action of *Shm5*$^{TEN1/TEN1}$ when the genotype is *Shm3*$^{TEN1/TEN1}$, *Shm4*$^{C3H/-}$, and also *Shm5*$^{TEN1/TEN1}$ State of allele is unknown

[a] Results from Gotoh et al. (2012)

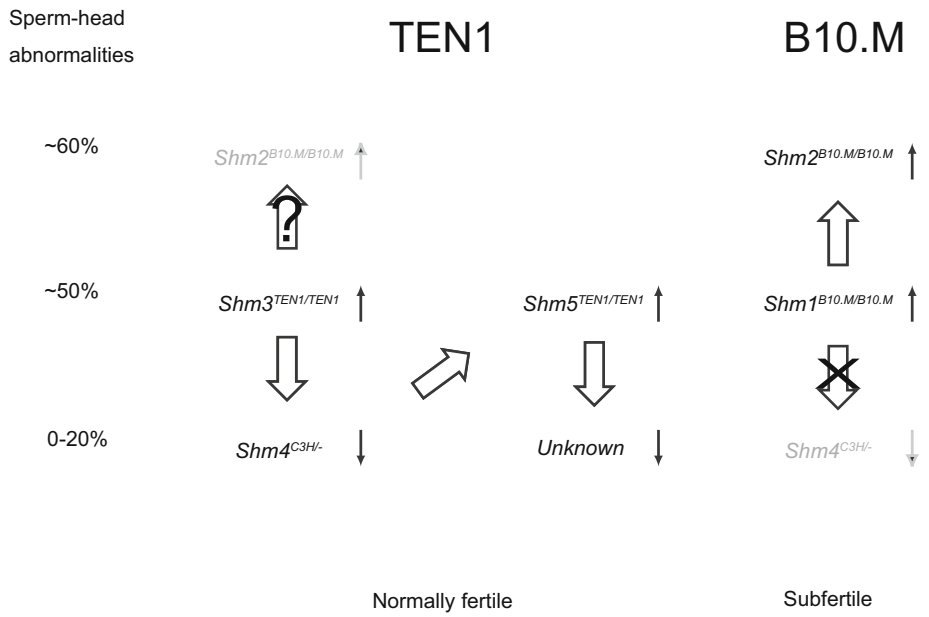

Fig. 5 Schematic models of polygenic regulation of sperm-head abnormalities in B10.M and TEN1 strains of mouse. *Italic letters* represent the genotype of the each locus. *Thin arrows* next to the genotypes show the actions of the genotypes regarding to the frequencies of sperm-head abnormalities. *Thick arrows* show the sequential polygenic interactions of the loci involved. As C3H strain was used for genetic analysis of the B10.M strain (Gotoh et al. 2012), the *Shm4*$^{C3H/-}$ has been confirmed to have no effect to the *Shm1*$^{B10.M/B10.M}$ genotype. Interaction between the *Shm3*$^{TEN1/TEN1}$ and the *Shm2*$^{B10.M/B10.M}$ has not been tested

function of *Shm5*^{TEN1} to suppress the action of *Shm4*$^{C3H/-}$ conditionally (Table 3). However, 48 % of the animals genotyped as *Shm3*$^{TEN1/TEN1}$, *Shm4*$^{C3H/-}$, and *Shm5*$^{TEN1/TEN1}$ showed low frequency of sperm-head abnormalities, contrary to our expectation (Fig. 3; Table 2). Another locus that suppresses the action of *Shm5*$^{TEN1/TEN1}$ should be present. The interacting genetic element may not be solitary. Further interpretation became difficult because the sample size of this study ($n = 592$) was not sufficient.

Because TEN1 strain is the *H2* congenic strain, we predicted that the gene responsible for the abnormal sperm-head phenotype was located on Chr 17. However, the responsible loci were mapped outside of the *H2* complex on Chr 17. The origin of *Shm3*^{TEN1} and *Shm5*^{TEN1} mutations is speculated to have either transferred from the progenitor wild mouse, the donor of the *H2* complex of TEN1, or to have emerged *de novo* during the establishment of the TEN1 strain. Although both *Shm1*$^{B10.M}$ and *Shm3*^{TEN1} were

mapped within the identical region on Chr 1, it was considered to be a coincidence because both the TEN1 and B10.M strains were developed independently at the National Institute of Genetics, Japan (Shiroishi et al. 1982) and at the Jackson Laboratory (Snell and Jackson, 1958), respectively.

From our studies using mutant strains showing teratozoospermia, epistatic interactions of *Shm* loci became apparent. Both the TEN1 and the B10.M strains are the useful tools for determining responsible genes for teratozoospermia. However, epistasis on teratozoospermia has been shown to be a common feature in the laboratory mice. In the study to observe sperm-head abnormalities in F2 animals produced between C3H/HeN and C57BL/6 J strains, involvement of numerous loci for teratoazoospermia has been reported (Gotoh and Aoyama, 2012). The observation that $\sim$4 % of animals showed unexpected values for the frequency of sperm-head abnormalities in this study (Fig. 3; Table 2) can be interpreted in the same context. The involvement of epistasis in mouse reproductive performance has been reported in other studies (Peripato et al. 2004; Flachs et al. 2012). Our findings further confirm the notion that the reproductive system is controlled by the coordinated action of numerous genes.

Although TEN1 strain shows both teratozoospermia and considerable histological changes in testis, its male reproductive performance was observed normal. On the other hand, B10.M strain shows teratozoospermia and male subfertility (Hirawatari et al. 2015). Relationship between abnormal sperm morphology and male subfertility in B10.M strain has not been established. Identification of responsible gene(s) for B10.M male subfertility is necessary to clarify the important issue of reproduction.

Acknowledgments The authors acknowledge the assistance of Mr. Heiichi Uchiyama with the experiments. We thank Dr. Shiroishi for providing the B10.MOL-TEN1 mouse strain. This work was supported by the Ministry of Agriculture, Forestry, and Fisheries, Japan.

References

Aitken RJ (2006) Sperm function tests and fertility. Int J Androl 29(1):69–75

Browman KW, Sen S (2009) A guide to QTL mapping with R/qtl. Springer, New York

Browman KW, Wu H, Sen S, Churchill GA (2003) R/qtl: QTL mapping in experimental crosses. Bioinformatics 19(7):889–890

Flachs P, Mihola O, Simeček P, Gregorová S, Schimenti JC, Matsui Y, Baudat F, de Massy B, Piálek J, Forejt J, Trachtulec Z (2012) Interallelic and intergenic incompatibilities of the Prdm9 (Hst1) gene in mouse hybrid sterility. PLoS Genet 8(11):e1003044

Furuse T, Yamada I, Kushida T, Masuya H, Miura I, Kaneda H, Kobayashi K, Wada Y, Yuasa S, Wakana S (2012) Behavioral and neuromorphological characterization of a novel Tuba1 mutant mouse. Behav Brain Res 227(1):167–174

Gotoh H (2010) Inherited sperm head abnormalities in the B10.M mouse strain. Reprod Fertil Dev 22(7):1066–1073

Gotoh H, Aoyama H (2012) Spermatogenic defects in F2 mice between normal mouse strains C3H and C57BL/6 without mutation. Congenit Anom (Kyoto) 52(4):186–190

Gotoh H, Hirawatari K, Hanzawa N, Miura I, Wakana S (2012) QTL on mouse chromosomes 1 and 4 causing sperm-head morphological abnormalities and male subfertility. Mamm Genome 23(7–8):399–403

Guzick DS, Overstreet JW, Factor-Litvak P, Brazil CK, Nakajima ST, Coutifaris C, Carson SA, Cisneros P, Steinkampf MP, Hill JA, Xu D, Vogel DL (2001) Sperm morphology, motility and concentration in fertile and infertile men. N Engl J Med 345(19):1388–1393

Handel MA, Lessard C, Reinholdt L, Schimenti J, Eppig JJ (2006) Mutagenesis as an unbiased approach to identify novel contraceptive targets. Mol Cell Endocrinol 250(1–2):201–205

Hirawatari K, Hanzawa N, Kuwahara M, Aoyama H, Miura I, Wakana S, Gotoh H (2015) Polygenic expression of teratozoospermia and normal fertility in B10.MOL-TEN1 mouse strain. Congenit Anom (Kyoto) 55(2):92–98

Jamsai D, O'Bryan MK (2011) Mouse models in male fertility research. Asian J Androl 13(1):139–151

Lewis SE (2007) Is sperm evaluation useful in predicting human fertility? Reproduction 134(1):31–40

Lucy MC (2001) Reproductive loss in high-producing dairy cattle: where will it end? J Dairy Sci 84(6):1277–1293

Maas JA, Garnsworthy PC, Flint AP (2009) Modelling responses to nutritional, endocrine and genetic strategies to increase fertility in the UK dairy herd. Vet J 180(3):356–362

Massart A, Lissens W, Tournaye H, Stouffs K (2012) Genetic causes of spermatogenic failure. Asian J Androl 14(1):40–48

Matzuk MM, Lamb DJ (2008) The biology of infertility: research advances and clinical challenges. Nat Med 14(11):1197–1213

Oehninger S, Franken DR, Ombelet W (2014) Sperm functional tests. Fertil Steril 102(6):1528–1533

Oka A, Mita A, Sakurai-Yamatani N, Yamamoto H, Takagi N, Takano-Shimizu T, Toshimori K, Moriwaki K, Shiroishi T (2004) Hybrid breakdown caused by substitution of the X chromosome between two mouse subspecies. Genetics 166(2):913–924

Peripato AC, De Brito RA, Matioli SR, Pletscher LS, Vaughn TT, Cheverud JM (2004) Epistasis affecting litter size in mice. J Evol Biol 17(3):593–602

Royal MD, Smith RF, Friggens NC (2008) Fertility in dairy cows: bridging the gaps. Animal 2(8):1101–1103

Shiroishi T, Sagai T, Moriwaki K (1982) A new wild-derived H-2 haplotype enhancing K-IA recombination. Nature 300(5890): 370–372

Snell GD, Jackson RB (1958) Histocompatibility genes of the mouse. II. Production and analysis of isogenic resistant lines. J Natl Cancer Inst 21(5):843–877

Storchová R, Gregorová S, Buckiová D, Kyselová V, Divina P, Forejt J (2004) Genetic analysis of X-linked hybrid sterility in the house mouse. Mamm Genome 15(7):515–524

Visser L, Repping S (2010) Unravelling the genetics of spermatogenic failure. Reproduction 139(2):230–253

Vyskocilová M, Prazanová G, Piálek J (2009) Polymorphism in hybrid male sterility in wild-derived Mus musculus musculus strains on proximal chromosome 17. Mamm Genome 20(2): 83–91

Wyrobek AJ, Gordon LA, Burkhart JG, Francis MW, Kapp RW, Letz G, Malling HV, Topham JC, Whorton MD (1983) An evaluation of the mouse sperm morphology test and other sperm test in nonhuman mammals. Mutat Res 115(1):1–72